Competing magnetic order in holmium-thulium superlattices

1998 J. Phys.: Condens. Matter 10 2115

(http://iopscience.iop.org/0953-8984/10/9/015)

J. Phys.: Condens. Matter **10** (1998) 2115–2124. Printed in the UK PII: S0953-8984(98)89565-9

Competing magnetic order in holmium–thulium superlattices

R A Cowley†, J A Simpson†, R C C Ward†, M R Wells† and D F McMorrow‡

† Oxford Physics, Clarendon Laboratory, Parks Road, Oxford OX1 3PU, UK
‡ Department of Solid State Physics, Risø National Laboratory, DK-4000 Roskilde, Denmark

Received 26 November 1997

Abstract. Superlattices of holmium and thulium have been grown using molecular beam epitaxy and their magnetic structures determined using neutron scattering techniques. At all temperatures below the Néel temperature of Ho, $T_N(\mathrm{Ho})$, the holmium moments form a basal-plane helix. Above $T_N(\mathrm{Tm})$ this helix is coherent across several bi-layer blocks even though there is no significant ordered moment in the intermediate thulium layers. Below approximately 50 K the thulium moments order, forming a longitudinally modulated structure similar to that of the bulk. For the $\mathrm{Ho_{40}/Tm_{10}}$ and $\mathrm{Ho_{20}/Tm_{20}}$ samples there is little coherence of the longitudinal thulium phase in successive blocks, while there is coherence of the holmium structure, although the magnetic coherence length decreases with decreasing temperature. In contrast, the $\mathrm{Ho_{10}/Tm_{40}}$ sample has coherent magnetic order between the thulium blocks with a lack of coherence in the structure formed in successive holmium blocks. These results are similar to those reported for holmium–erbium superlattices which are also superlattices of two elements which have competing crystal-field anisotropies.

1. Introduction

In recent papers [1–3], unusual effects have been reported for superlattices composed of two magnetic rare-earth metals. Earlier studies on magnetic/non-magnetic superlattices, such as dysprosium/yttrium ones [4], have established that the magnetic order propagates coherently through the non-magnetic blocks with a largely temperature-dependent coherence length of up to about 500 Å. The behaviour of the magnetic ordering in holmium–erbium superlattices is different. Instead of long-range magnetic order with an almost constant coherence length, the coherence length decreases with decreasing temperature when the magnetic moments of both the holmium and erbium atoms order. The ordering of the moments in the basal plane appears to compete with the ordering of the erbium moments along the *c*-axis. All of these samples showed this unusual characteristic. In more detail, a basal-plane helical ordering of the holmium forms below 133 K, the ordering temperature of bulk holmium, with order coherent over 600 Å, a distance of several superlattice repeats. On cooling, this structure persists until below about 84 K, when the erbium moments order incommensurately in both the basal plane and along the *c*-axis. The coherence length of the basal-plane ordering then decreases to a limit of about 200 Å at low temperatures, while the phase of the *c*-axis-modulated structure is uncorrelated from one erbium layer to the next.

The unexpected nature of this result has led us to investigate holmium–thulium superlattices, with the aim of furthering our understanding of the propagation of long-range order in rare-earth superlattices. (The background to our measurements is described

0953-8984/98/092115+10$19.50

in detail with the results for the holmium–erbium superlattices [2] and will not be repeated here in this short paper.) The holmium–thulium combination, like holmium and erbium, is one in which the two elements have competing crystal-field anisotropies. Furthermore, erbium has a relatively weak anisotropy, so for both the bulk and the superlattices, the magnetic moments have ordered components along both the c-axis and in the basal plane. In contrast, bulk thulium orders with the magnetic moments ferromagnetically aligned in each basal plane, but the moment direction is always along the c-axis [5]. This is largely because the crystal-field parameter B_2^0 is -0.096 meV for thulium [6], compared to a value of -0.027 meV for erbium [7]. The competition between crystal-field anisotropies in the basal plane and along the c-axis is therefore stronger for holmium–thulium superlattices than for holmium–erbium ones, and should provide more insight into the propagation of magnetic order in rare-earth superlattices.

Below 55 K, thulium orders magnetically, with the moments aligned ferromagnetically in each basal plane but the ferromagnetic moments forming a longitudinally modulated structure with a wave vector of 0.273 $\boldsymbol{c}^*$. On cooling, the wave vector increases to $0.286 = (2/7)\ \boldsymbol{c}^*$ at 30 K, below which it remains commensurate with a squared-up structure having alternately four 'up' moments and three 'down' moments. Holmium has an ordered magnetic structure below 133 K in which the moments are also ferromagnetically aligned in each basal plane, but the moments are aligned within the basal planes [8]. The structure is a basal-plane helix and the wave vector of the helix is 0.282 $\boldsymbol{c}^*$ on ordering and reduces to $0.167 = (1/6)\ \boldsymbol{c}^*$ on cooling. However, for a 10 000 Å film of holmium grown by MBE techniques, the moments order in a similar manner to the bulk, with the exception that the wave vector only reduces to approximately 0.2 $\boldsymbol{c}^*$ on cooling to low temperature [9].

Table 1. Structural properties of Ho/Tm superlattices at 10 K.

n_{Ho}	n_{Ho} fitted	n_{Tm}	n_{Tm} fitted	a (Å)	c_{Ho} (Å)	c_{Tm} (Å)
40	37.5 ± 2.0	10	9.5 ± 1.0	3.577 ± 0.01	2.806 ± 0.005	2.755 ± 0.01
20	17.0 ± 2.0	20	22.0 ± 2.0	3.564 ± 0.01	2.803 ± 0.005	2.764 ± 0.01
10	10.0 ± 1.0	40	37.5 ± 2.0	3.548 ± 0.01	2.800 ± 0.005	2.752 ± 0.01

2. Experimental details

Three samples of holmium–thulium superlattices were grown by the same techniques as for the holmium–erbium superlattices [2]. Nominally the samples were Ho_{40}/Tm_{10}, Ho_{20}/Tm_{20} and Ho_{10}/Tm_{40} where the subscripts refer to the number of atomic planes of each element within the bi-layer repeat, which was repeated 70 times. The superlattice repeat distances, the lattice parameters of the holmium and thulium and the number of planes of each were deduced from the neutron scattering measurements and are listed in table 1. The mosaic spreads of the superlattices were typically 0.4° FWHM, a value somewhat larger than obtained for the holmium–erbium superlattices. This is possibly because the differences in the lattice parameters of the bulk are larger for the holmium–thulium combination. The neutron scattering experiments were performed at the DR3 reactor of the Risø National Laboratory using the triple-axis spectrometer, TAS6. The collimators were selected to give a wave-vector resolution of approximately 0.017 Å^{-1} for elastically scattered 5 meV neutrons, and the contamination from higher-order neutrons was reduced by employing a cooled Be filter. The samples were mounted in a closed-cycle cryostat, and the temperature was controlled between 300 K and 10 K to ±0.1 K and the $(h0l)$ crystallographic plane was aligned in the scattering plane of the spectrometer. Scans of the wave-vector transfer were performed along the [00l] and [10l] directions. The results from the measurements are discussed below, with those from [00l] scans considered first because they provide directly information about the ordering of the magnetic moments in the basal plane. The scattering observed with the [10l] scans arises from the ordering of the magnetic moments in both the basal plane and along the c-axis. The magnetic ordering along the c-axis is then obtained by subtracting the component of the scattering due to the basal-plane ordering from the [10l] data. Finally the variation in the coherence length of the different types of ordering will be described.

Table 2. Basal-plane magnetic ordering of Ho/Tm superlattices at 10 K.

n_{Ho}	n_{Tm}	q_{Ho} (c^*)	q_{Tm} (c^*)	ξ (Å)	μ_{Ho} (μ_B)
40	10	0.200 ± 0.003	0.286 ± 0.01	498 ± 30	9.8 ± 0.5
20	20	0.200 ± 0.003	0.282 ± 0.005	230 ± 30	9.9 ± 0.5
10	40	0.201 ± 0.005	—	32 ± 5	7.4 ± 0.5

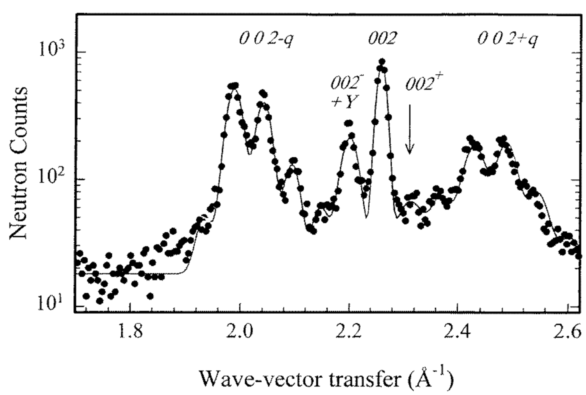

Figure 1. The neutron scattering observed from a Ho_{20}/Tm_{20} superlattice at 10 K when the wave-vector transfer was varied along the [00l] direction. The nuclear scattering from the (002) Bragg reflection of the superlattice and Y seed are shown near 2.2 Å^{-1} and the magnetic scattering near 2.0 and 2.4 Å^{-1}. The solid line is the result of a fit to the model described in the text.

3. Experimental results

A typical example of the scattered neutron intensity observed while the wave-vector transfer is varied along the [00l] direction is shown in figure 1 for the Ho_{20}/Tm_{20} sample at a temperature of 10 K. The scattering shows a series of sharp peaks which are characteristic of the scattering from a superlattice and arise from nuclear Bragg scattering and from scattering by a helical magnetic structure which extends coherently over several superlattice blocks. Similar results were obtained for the Ho_{40}/Tm_{10} sample. These results were

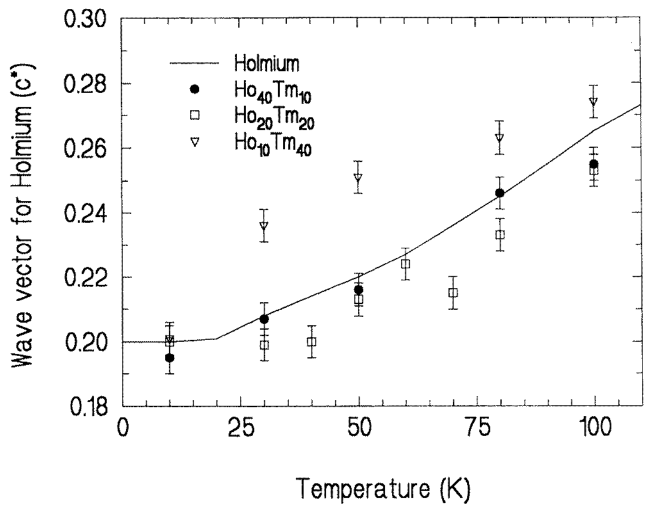

Figure 2. The wave vector describing the turn angle of the magnetic ordering between the Ho planes for the basal-plane ordering of Ho/Tm superlattices. The solid line shows the turn angle of a similar 5000 Å film [7].

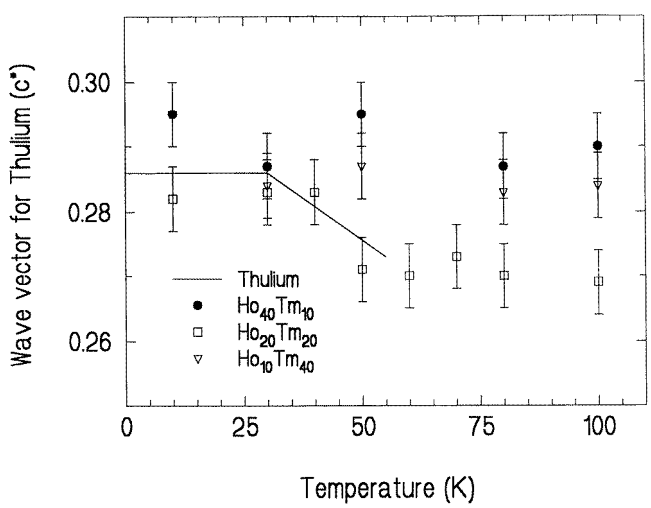

Figure 3. The wave vector describing the effective turn angle between the Tm planes for the basal-plane ordering of Ho/Tm superlattices. The solid line shows the wave vector of the ordering of bulk Tm.

therefore analysed using the same model as successfully accounted for the scattering from holmium–yttrium [9] and holmium–erbium [1, 2] superlattices. The magnetic scattering was assumed to arise from a basal-plane helix for the holmium layers with the helical turn angle described by the wave vector, q_{Ho}, and a similar helical wave vector, q_{Tm}, for the thulium. The parameters of this model were obtained by a least-squares fit of this model to the experimental results and the resulting fit is shown by the solid line in figure 1. The results for the wave vectors, q_{Ho} and q_{Tm}, are illustrated in figures 2 and 3, while figure 4

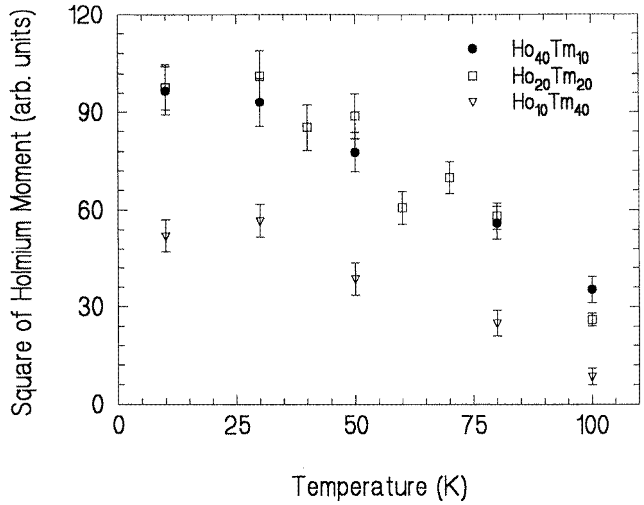

Figure 4. The square of the ordered moment in the basal-plane for Ho atoms as a function of temperature for the Ho/Tm superlattices.

shows the square of the amplitude of the holmium ordered moment. The main features of the results are that q_{Tm} is within error independent of temperature, largely independent of the superlattice, and similar to the corresponding wave vector of the bulk, which is shown by the solid line in figure 3. The wave vector q_{Ho} is temperature dependent and for the two superlattices containing the most holmium is similar to q_{Ho} for a film of holmium grown by the same method and having a thickness of 5000 Å [9], as shown in figure 2. The parameters of the fits gave no significant ordered basal-plane component for the thulium layers, and the temperature dependence of the square of the ordered holmium moment is shown in figure 4. The absolute magnitudes of the ordered moments at 10 K were obtained by comparing the intensity of the magnetic scattering with that of the (002) Bragg reflection and allowing for the Lorenz factor and the wave-vector dependence of the form factor. The results are summarized in table 2, and for the $\mathrm{Ho_{20}/Tm_{20}}$ and $\mathrm{Ho_{40}/Tm_{10}}$ samples the moments are in excellent agreement with the value of 10 μ_B expected for the holmium atoms. This result taken together with the absence of a marked change in the intensity near the temperature at which bulk thulium orders, and the overall quality of the fits to the experimental results, supports the conclusion that the thulium layers do not have ordered magnetic moments in the basal plane.

The overall results for [00*l*] scattering from the $\mathrm{Ho_{10}/Tm_{40}}$ sample are different from those of the other two superlattices. At temperatures above 55 K, the scattering is similar to that from the other samples, and consistent with holmium forming a basal-plane helical structure and with no order on the thulium layers. However, the coherence length is much shorter than that found for the other holmium-rich samples and this may be due to the large number of thulium planes in each block. The coherence length in the non-magnetic/magnetic superlattices also decreases as the thickness of the non-magnetic layer increases [4]. The data above 55 K could be satisfactorily fitted using the same model as that described above, and the results are shown in figures 2–4. The results for q_{Tm} are similar to those of the other superlattices but those for q_{Ho} are significantly larger except for $T = 10$ K. The ordered moment for the holmium atoms for the $\mathrm{Ho_{10}/Tm_{40}}$ sample is smaller than for the other

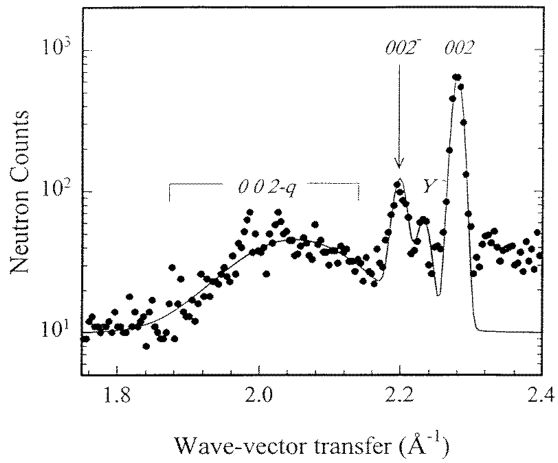

Figure 5. The neutron scattering observed from a Ho_{10}/Tm_{40} superlattice at 10 K with the wave-vector transfer along the [00*l*] direction. The broad magnetic scattering is labelled as at $(0\,0\,2 - q)$. The solid line is a fit to a series of Gaussians.

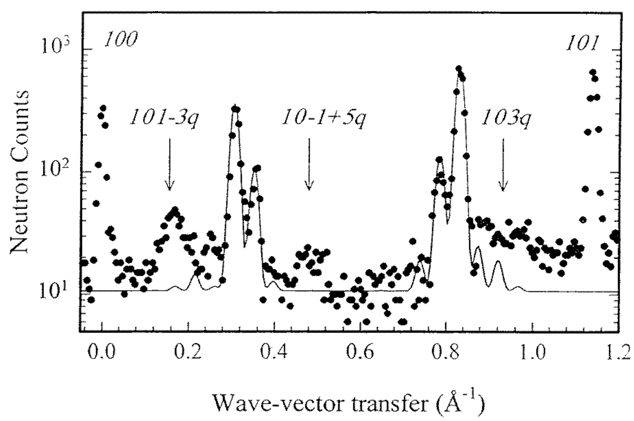

Figure 6. The neutron scattering observed from a Ho_{10}/Tm_{40} superlattice at 10 K with the wave-vector transfer along the [10*l*] direction. The solid line shows a fit to the first-order scattering from a coherent longitudinally modulated structure. The nuclear Bragg peaks are at (100) and (101) and the third- and fifth-order harmonics are also indicated.

superlattice. Below 55 K, the [00l] scattering is markedly different from that of the other superlattices, as illustrated in figure 5. This profile has been analysed in two ways: by fitting a single, broad Gaussian function, or to a series of sharper Gaussians to reproduce the small peaks which are apparent in the scattering. The broad peak has a width consistent with the scattering from a single Ho block and the scattering predicted by this hypothesis is shown by the solid line in figure 5. Fits using several sharper peaks have a spacing in wave vector between the peaks which is inconsistent with the scattering from a coherent magnetic structure for the superlattice. The widths of the peaks correspond to a coherence length of about 1.5 bi-layers. The data do not enable us to distinguish between these two models and so there are relatively large error bars for the parameters of the basal-plane ordering for this sample. Table 2 and figure 4 also show that the basal-plane component of the ordered

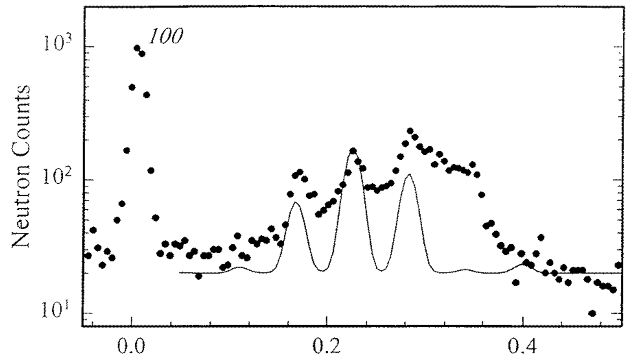

Figure 7. The neutron scattering observed from a Ho_{20}/Tm_{20} superlattice at 10 K with the wave-vector transfer along the [10l] direction. The solid line shows a calculation of the contribution to the magnetic scattering from the basal-plane ordering and was calculated using the model deduced from the scattering observed along the [00l] direction.

holmium moment of is only about 0.77 ± 0.10 of the moment observed for bulk holmium and the other superlattices. The general agreement between the nominal number of atomic layers and the parameters obtained from the fitting to the experiments for all of the samples (shown in table 1) give confidence that we have not overestimated the thickness of the Ho blocks for the Ho_{10}/Tm_{40} sample. We suggest that the holmium moment is not fully aligned in the basal plane and may be either partially disordered or partially aligned along the c-axis by exchange interactions with the ordered thulium moments. The scattering observed when the wave-vector transfer is varied along the [10l] direction is shown for the Ho_{10}/Tm_{40} and Ho_{20}/Tm_{20} samples in figures 6 and 7 respectively. As found for the [00l] direction, the nature of the [10l] scattering from the Ho_{10}/Tm_{40} sample is different from that of the other two samples. All of the results show temperature-independent scattering from the (100) Bragg reflection and so there is no evidence of ordering with a ferromagnetic c-axis component. The cone phase, which occurs at low temperatures for bulk holmium, does not occur for these Ho/Tm superlattices. This is possibly because the substrate of the superlattice clamps the basal plane and this clamping inhibits the magneto-elastic contribution to the anisotropy. The stability of the cone phase is thereby suppressed, as observed for other holmium superlattices and thin films [9].

Table 3. Longitudinal magnetic ordering of Ho/Tm superlattices at 10 K.

n_{Ho}	n_{Tm}	q_{Ho} (c^*)	q_{Tm} (c^*)	ξ (Å)	μ_{Tm} (μ_B)
40	10	—	0.285 ± 0.02	—	6.5 ± 2.0
20	20	—	0.277 ± 0.005	50 ± 10	7.5 ± 1.0
10	40	0.239 ± 0.005	0.279 ± 0.005	547 ± 30	7.4 ± 1.0

The remaining [10l] results will be described by considering the Ho_{10}/Tm_{40} sample first. The scattering at low temperature, 10 K, is shown in figure 6 and has sharp peaks characteristic of the scattering from a coherent superlattice structure. Since the contribution of the basal-plane moments to the [10l] scattering is relatively small and broad, these results were analysed on the assumption that the sharp peaks arise from scattering from ordering in a largely coherent longitudinally modulated structure. The results for the thulium and holmium wave vectors are listed in table 3 and can be compared with wave vectors deduced from the basal-plane scattering in table 2. Within the considerable errors, the turn angles were independent of temperature up to the ordering temperature of bulk thulium. In addition, figure 6 shows some broader peaks which can be identified with the higher harmonics $(1\,0\,1-3q)$ and $(1\,0\,{-1}+5q)$. Similar scattering was observed for bulk thulium [5] for which the ratios of the intensities $I(1-3q)/I(q)$ and $I(5q-1)/I(q)$ near the (100) Bragg reflection were 0.37 and 0.17 respectively at $T = 10$ K. For the superlattice these ratios are $0.31+0.05$ and $0.06+0.02$ respectively, which are similar to those of the bulk. Close agreement with the bulk behaviour is also obtained for the thulium moment: a value of 7.4 μ_B is obtained from the intensity of the magnetic scattering of the superlattice (table 2) whereas the expected moment of a thulium atom is 7 μ_B. These two results suggest that the magnetic structure of the thulium in this superlattice is very similar to that of bulk thulium. The widths of the $3q$- and $5q$-peaks are shown in figure 6 and are approximately consistent with the widths expected for the scattering from isolated thulium blocks. We conclude that although there is long-range coherence for the primary harmonic of the scattering, the phase of the higher harmonics is uncorrelated from one thulium block to the next.

The scattering observed from the Ho_{20}/Tm_{20} sample when the wave-vector transfer was varied along the [10*l*] direction is shown in figure 7. This result is more difficult to interpret than that shown in figure 6 because the scattering from the basal-plane ordering is a substantial fraction of the observed scattering. Above 55 K, the models deduced from the [00*l*] data can completely account for the observed scattering along [10*l*], and so we conclude that there is then no longitudinal ordering of the moment along the *c*-axis above 55 K. At lower temperatures there is additional intensity, as shown in figure 7, which is consistent with a broad peak with a width similar to that expected for the scattering from a single Tm block and centred at the wave vector listed in table 3. A quantitative analysis of this broad peak is complicated by the possible presence of third- and fifth-order harmonics of the scattering. Similar results were obtained for the Ho_{40}/Tm_{10} sample but the subtraction procedure is even more difficult in this case because the longitudinal scattering is a smaller fraction of the total scattering. The results of the analysis for q_{Tm} and the thulium moment are listed in table 3.

The coherence lengths of the magnetic structures were obtained from the width of the scattering peaks by fitting a Gaussian form, $\exp(-q^2/(2\sigma^2))$, and then subtracting the resolution width from the σ by assuming that the widths added in quadrature. The coherence length was then taken as the FWHM of the Gaussian profile, namely $L = 2.33/\sigma$, and the results for the coherence length of the basal-plane ordering are shown in figure 8. For the Ho_{40}/Tm_{10} and Ho_{20}/Tm_{20} samples the coherence length is several bi-layers, and indeed in the case of the former superlattice it was so long that it could not be reliably measured. On cooling below the ordering temperature of bulk thulium the coherence length reduces steadily to between 1.5 and 3 bi-layers at low temperature. This shows that the development of the longitudinal ordering of the thulium layers causes a decrease in the coherence length of the basal-plane ordering. The thulium moments order along the *c*-axis, and for these samples there is no evidence for any coherence in that ordering from one bi-layer to the next. This behaviour is qualitatively identical to that found for the coherence length of the holmium/erbium superlattices [1, 2].

The coherence of the structures of the Ho_{10}/Tm_{40} sample is different. At temperatures above 55 K the basal-plane ordering is coherent for only 1.5 bi-layers, showing that as the thickness of thulium increases the coherence of the basal-plane holmium helix decreases. The coherence of the basal-plane ordering at low temperatures is less certain, but the

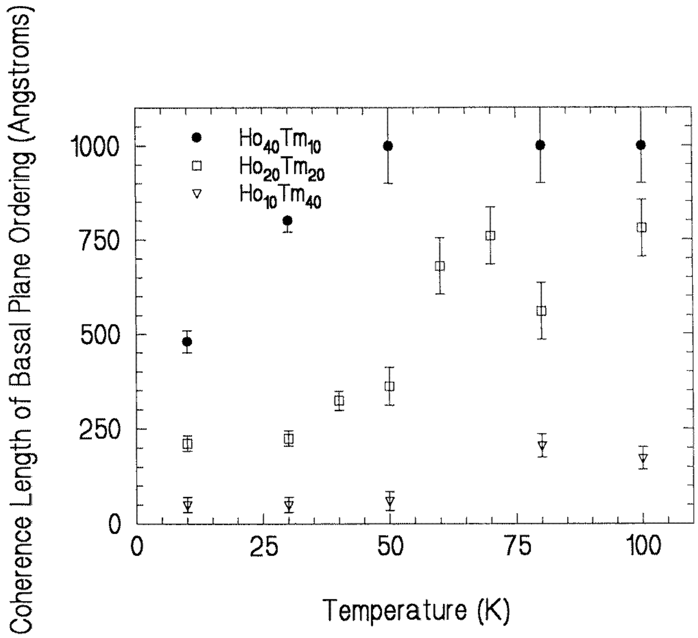

Figure 8. The coherence length of the basal-plane ordering of Ho/Tm superlattices. The coherence length of the Ho_{40}/Tm_{10} sample above 50 K is larger than 1000 Å and has not been measured.

scattering shows that the coherence length decreases below 50 K until there is little or no coherence between the magnetic ordering of different holmium blocks at 10 K. The longitudinal ordering of the thulium moments has a coherence length of 3 bi-layers at 50 K and this increases to 4 bi-layers at 10 K. These results suggest that in this sample the longitudinal ordering of the thulium dominates, and destroys the weaker coherence of the holmium basal-plane ordering. At 10 K, the longitudinal ordering has a coherence length similar to that of the basal-plane ordering of the Ho_{40}/Tm_{10} sample. In comparison, the holmium/erbium superlattices do not exhibit coherence of the longitudinal ordering, presumably because the longitudinal anisotropy of erbium is weaker than that of thulium.

In conclusion we have measured the magnetic structures of holmium–thulium superlattices using neutron scattering techniques. The results are similar to those of holmium–erbium superlattices in which the constituent elements also have competing anisotropies. They show that the magnetic structures have long-range coherence over several bi-layer repeats below the ordering temperature of bulk holmium but above that of bulk thulium. In this temperature range the magnetic structure is a basal-plane helix with ordering of the holmium moments. Below the ordering temperature of bulk thulium, the coherence length of the basal-plane ordering decreases with decreasing temperature. For the holmium-rich samples there is a modulated longitudinal ordering of the thulium layers, but this ordering is not coherent between successive thulium layers. In the thulium-rich sample the longitudinal ordering dominates and establishes a coherent structure while the coherence of the basal-plane ordering of successive holmium layers is destroyed. These results confirm the conclusion drawn from the study of holmium–erbium superlattices [1, 2], namely that two different types of magnetic ordering cannot simultaneously establish structures which are coherent over several bi-layers.

Acknowledgments

We have benefited from helpful discussions with C Bryn-Jacobsen, J Jensen and the late A R Mackintosh. Financial support was provided in Oxford by the EPSRC, and in Risø by the EU through the Large Installations Programme.

References

[1] Simpson J A, McMorrow D F, Cowley R A, Jehan D A, Ward R C C, Wells M R and Clausen K N 1994 *Phys. Rev. Lett.* **73** 1162
[2] Simpson J A, Cowley R A, Jehan D A, Ward R C C, Wells M R, McMorrow D F, Clausen K N, Thurston T R and Gibbs D 1996 *Z. Phys.* B **101** 35
[3] Dumensil K, Dufour C, Mangin Ph, Marchal G and Hennion M 1996 *Phys. Rev.* B **54** 6407
[4] Rhyne J J, Erwin R W, Borchers J, Matheny A, Sinha S, Salamon M B, Du R and Flynn C P 1987 *J. Appl. Phys.* **61** 4043
[5] Koehler W C, Cable J W, Wollan E O and Wilkinson M K 1962 *Phys. Rev.* **126** 1672
[6] McEwen K A, Steigenberger U and Jensen J 1991 *Phys. Rev.* B **43** 3298
[7] Cowley R A and Jensen J 1993 *J. Phys.: Condens. Matter* **4** 9673
[8] Koehler W C, Cable J W, Wilkinson M K and Wollan E O 1966 *Phys. Rev.* **151** 414
[9] Jehan D A, McMorrow D F, Cowley R A, Ward R C C, Wells M R and Hagman N 1993 *Phys. Rev.* B **48** 5594